World Journal of Gastroenterology

Online Submissions: http://www.wjgnet.com/esps/
wjg@wjgnet.com
doi:10.3748/wjg.v19.i24.3792

World J Gastroenterol 2013 June 28; 19(24): 3792-3801
ISSN 1007-9327 (print) ISSN 2219-2840 (online)

ORIGINAL ARTICLE

Annexin A2 silencing inhibits invasion, migration, and tumorigenic potential of hepatoma cells

Hai-Jian Zhang, Deng-Fu Yao, Min Yao, Hua Huang, Li Wang, Mei-Juan Yan, Xiao-Di Yan, Xing Gu, Wei Wu, Shao-Lin Lu

Hai-Jian Zhang, Deng-Fu Yao, Min Yao, Li Wang, Mei-Juan Yan, Wei Wu, Shao-Lin Lu, Research Centre of Clinical Medicine, Affiliated Hospital of Nantong University, Nantong 226001, Jiangsu Province, China
Hua Huang, Department of Pathology, Affiliated Hospital of Nantong University, Nantong 226001, Jiangsu Province, China
Xiao-Di Yan, Xing Gu, Department of Clinical Oncology, Affiliated Hospital of Nantong University, Nantong 226001, Jiangsu Province, China
Author contributions: Zhang HJ and Yao M contributed equally to this work, designed the research study, conducted the experiments, analysed the data, and wrote the paper; Wang L, Yan MJ and Gu X carried out the *in vitro* experiments; Wu W and Yan XD performed the *in vivo* experiments; Huang H conducted the immunohistochemical and hematoxylin and eosin staining analyses; Lu SL critically reviewed the manuscript; Yao DF is the guarantor.
Supported by The Society Development of Nantong, No. HS2012034; the Jiangsu Health Projects, No. BL2012053 and No. K201102; the Priority Academic Program Development of Jiangsu, and the International S and T Cooperation Program of China, No. 2013DFA32150
Correspondence to: Deng-Fu Yao, MD, PhD, Professor, Research Centre of Clinical Medicine, Affiliated Hospital of Nantong University, 20 West Temple Road, Nantong 226001, Jiangsu Province, China. yaodf@ahnmc.com
Telephone: +86-513-85052297 Fax: +86-513-85052254
Received: March 13, 2013 Revised: April 30, 2013
Accepted: May 18, 2013
Published online: June 28, 2013

Abstract

AIM: To investigate the effects of Annexin A2 (ANXA2) silencing on invasion, migration, and tumorigenic potential of hepatoma cells.

METHODS: Human hepatoma cell lines [HepG2, SMMC-7721, SMMC-7402, and MHCC97-H, a novel human hepatocellular carcinoma (HCC) cell line with high metastasis potential] and a normal hepatocyte cell line (LO2) were used in this study. The protein and mRNA expression levels of ANXA2 were analysed by western blotting and real-time polymerase chain reaction, respectively. The intracellular distribution profile of ANXA2 expression was determined by immunofluorescence and immunohistochemistry. Short hairpin RNA targeting ANXA2 was designed and stably transfected into MHCC97-H cells. Cells were cultured for *in vitro* analyses or subcutaneously injected as xenografts in mice for *in vivo* analyses. Effects of ANXA2 silencing on cell growth were assessed by cell counting kit-8 (CCK-8) assay (*in vitro*) and tumour-growth assay (*in vivo*), on cell cycling was assessed by flow cytometry and propidium iodide staining (*in vitro*), and on invasion and migration potential were assessed by transwell assay and wound-healing assay, respectively (both *in vitro*).

RESULTS: The MHCC97-H cells, which are known to have high metastasis potential, showed the highest level of ANXA2 expression among the four HCC cell types examined; compared to the LO2 cells, the MHCC97-H expression level was 8-times higher. The ANXA2 expression was effectively inhibited (about 80%) by ANXA2-specific small hairpin RNA (shRNA). ANXA2 expression in the MHCC97-H cells was mainly localized to the cellular membrane and cytoplasm, and some localization was detected in the nucleus. Moreover, the proliferation of MHCC97-H cells was obviously suppressed by shRNA-mediated ANXA2 silencing *in vitro*, and the tumour growth inhibition rate was 38.24% *in vivo*. The percentage of MHCC97-H cells in S phase dramatically decreased (to 27.76%) under ANXA2-silenced conditions. Furthermore, ANXA2-silenced MHCC97-H cells showed lower invasiveness (percentage of invading cells decreased to 52.16%) and suppressed migratory capacity (migration distance decreased to 63.49%). It is also worth noting that shRNA-mediated silencing of ANXA2 in the MHCC97-H cells led to abnormal apoptosis.

CONCLUSION: shRNA-mediated silencing of ANXA2

suppresses the invasion, migration, and tumorigenic potential of hepatoma cells, and may represent a useful target of future molecular therapies.

Key words: Annexin A2; Small hairpin RNA; Hepatocellular carcinoma; Invasion; Migration; Tumorigenic potential

Core tip: The overexpression of annexin A2 (ANXA2) is closely related to the high metastasis potential and invasion ability of HCC cells, and ANXA2 deficiency inhibits the invasion, migration, and tumorigenic potential of hepatocellular carcinoma (HCC) cells, which not only provides further insight into the pathogenesis of HCC but also provides a potential predictive biomarker for HCC prognosis and a potential therapeutic target.

Zhang HJ, Yao DF, Yao M, Huang H, Wang L, Yan MJ, Yan XD, Gu X, Wu W, Lu SL. Annexin A2 silencing inhibits invasion, migration, and tumorigenic potential of hepatoma cells. *World J Gastroenterol* 2013; 19(24): 3792-3801 Available from: URL: http://www.wjgnet.com/1007-9327/full/v19/i24/3792.htm DOI: http://dx.doi.org/10.3748/wjg.v19.i24.3792

INTRODUCTION

Hepatocellular carcinoma (HCC) is currently the 3rd leading cause of cancer-related death, and its worldwide incidence is increasing; epidemiologic studies have revealed a strong association between HCC and chronic liver disease and cirrhosis[1,2]. Surgical therapy with liver transplantation or resection remains the mainstay of curative therapy for patients in the early stage of HCC[3,4]. However, even with radical resection, 60%-70% of patients develop metastasis and experience recurrence within 5 years of surgery[5-7]. Although several clinicopathologic features have been identified as contributing factors to this disease's poor prognosis (*e.g.,* poorly-differentiated phenotype, large-sized tumour, and portal venous invasion), the underlying mechanisms of HCC development remain unclear[8,9]. Gaining a detailed understanding of the molecular processes of HCC will likely identify specific diagnostic and prognostic markers and facilitate development of novel targeted therapeutic strategies. To this end, recent studies have identified annexin A2 (ANXA2) as an important mediator of malignant transformation and development of HCC[10,11].

As one of the best characterized components of the annexin family, ANXA2 is a calcium-dependent phospholipid-binding protein[12,13]. Up-regulation of ANXA2 expression and its phosphorylation at tyrosine 23 (mediated by c-Src) has been observed in clinical samples of human HCC[14]; in addition, the tyrosine 23 phosphorylation-dependent cell-surface localization of ANXA2 was found to be required for the invasive and metastatic properties of pancreatic cancer[15]. Further studies of this ability to promote tumour metastasis have elucidated the molecular process in which ANXA2 induces plasminogen conversion to plasmin, thereby leading to activation of metalloproteinases, degradation of extracellular matrix components, and promotion of neoangiogenesis[10,16-18]. Thus, ANXA2-targeted interference by small hairpin RNA (shRNA) may represent an effective therapeutic strategy to mediate the biological behaviours of hepatoma cells.

In the present study, ANXA2 overexpression was found in MHCC97-H cells, a novel human HCC cell line with high metastasis potential, which was then used to investigate the effects of ANXA2 silencing on cell invasion, migration, and tumorigenic potential of HCC cells.

MATERIALS AND METHODS

Plasmid construction

ANXA2-specific shRNA targeting nucleotides 94-113 downstream of the transcription start site of ANXA2 was synthesized as previously described[16] and used to construct an experimental plasmid (pRNAT-U6.1-shRNA) by inserting into a *BamH* I -*Hind*Ⅲ linearized pRNAT-U6.1/Neo shRNA expression vector (Biomics Biotechnologies Co., Ltd., Nantong, China). A negative control vector (pRNAT-U6.1-negative) was constructed similarly with a shRNA sequence that does not suppress the expression of genes expressed in humans, rats, or mice (Biomics Biotechnologies Co., Ltd.). All inserted sequences were verified by DNA sequencing.

Cell culture and transfection

Human hepatoma cell lines (HepG2, SMMC-7721, and SMMC-7402) and a normal hepatocyte cell line (LO2) were obtained from Biomics Biotechnologies Co., Ltd. The MHCC97-H cell line was obtained from the Liver Cancer Institute of the Affiliated Zhongshan Hospital of Fudan University (Shanghai, China). For all cell lines, maintenance growth was carried out in Dulbecco's modified Eagle's medium (DMEM; Life Technologies, Inc., Frederick, MD, United States) supplemented with 10% foetal bovine serum (FBS) at 37 ℃ in a humidified atmosphere of 5% CO_2/95% air.

For experimentation, the MHCC97-H cells were seeded into 6-well plates, allowed to grow to 90%-95% confluence, and transfected with the plasmids (pRNAT-U6.1-negative or pRNAT-U6.1-shRNA) using PolyJet™ *In Vitro* DNA Transfection Reagent (SignaGen Laboratories, Gaithersburg, MD, United States) according to the manufacturer's instructions. At 48 h after transfection, cells were selected by culturing in the presence of 400 μg/mL of G418 (Life Technologies, Inc.) for 2 wk followed by 200 μg/mL of G418 for an additional 2 wk. Individual G418-resistant monoclonals were obtained by performing a limiting dilution with subsequent proliferation in medium supplemented with 200 μg/mL of G418 to generate the stably transfected experimental (MHCC97-H/

ANXA2-shRNA) and control (MHCC97-H/control-shRNA) cell lines.

RNA isolation and cDNA synthesis

Total RNA was isolated from mouse liver tissue specimens (50 mg) using the TRIzol Reagent (Life Technologies, Inc.) according to the manufacturer's instructions. Integrity of the isolated RNA was qualitatively assessed by 1% agarose gel electrophoresis and quantitatively assessed by ultraviolet spectrophotometry (absorbance at 260 nm, A_{260}; SmartSpec™ Plus; Bio-Rad Life Science Research and Development Co., Ltd., Shanghai, China); purity of the isolated RNA was indicated by an absorbance ratio at $A_{260/280}$ of < 1.8. The total RNA (1 μg) was applied as template for cDNA synthesis using the First-Strand cDNA Synthesis Kit (Fermentas Inc., Burlington, Canada) and following the manufacturer's instructions.

Quantitative real-time polymerase chain reaction

The cDNA samples (4 μg in 4 μL) were subjected to quantitative real-time polymerase chain reaction (qPCR) using an Applied Biosystems StepOne™ Real-Time PCR System (Life Technologies, Inc.) with the manufacturer's recommended protocol. The reaction solution (50 μL) contained 25 μL of 2 × SYBR Premix ExTaq (Takara Biotechnology Co., Ltd., Dalian, China), 2 μL of gene-specific primers, 1 μL of 50 × ROX Reference Dye I , and 18 μL deionized water. The following primers were used: ANXA2: forward, 5'-TGAGCGGGATGCTTTGAAC-3' and reverse, 5'-ATCCTGTCTCTGTGCATTGCTG-3'; β-actin (internal control): forward, 5'-ATTGCCGACAGGATGCAGA-3' and reverse, 5'-GAGTACTTGCGCTCAGGAGGA-3'[16]. Negative control reactions with no template (deionized water) were also included in each run. The optimized PCR conditions were: one cycle at 95 ℃ for 2 min; 40 cycles at 95 ℃ for 10 s, 62 ℃ for 1 min; 1 cycle at 72 ℃ for 2 min. The relative quantitative analysis was performed by comparison of the $2^{-\Delta\Delta Ct}$ values.

Western blotting

Total cell protein was extracted by sonication with 2 × sample buffer (0.25 mol/L Tris-HCl, 10% 2-mercaptoethanol, 4% sodium dodecyl sulphate (SDS), and 10% sucrose). Protein concentration was determined using the Enhanced Bicinchoninic Acid Protein Assay Kit (Beyotime Institute of Biotechnology, Haimen, China). Samples (20 μg) were resolved by 15% SDS-polyacrylamide gel electrophoresis and transferred onto polyvinylidene fluoride membranes. After blocking with 5% bovine serum albumin (BSA; Sigma-Aldrich, St. Louis, MO, United States) in Tris-buffered saline (pH 7.5; 100 mmol/L NaCl, 50 mmol/L Tris, and 0.1% Tween-20), the membranes were immunoblotted overnight at 4 ℃ with monoclonal primary antibody rabbit anti-human ANXA2 (1:500 dilution) and monoclonal primary antibody mouse anti-human β-actin (1:500) antibodies (Santa Cruz Biotechnology, Inc., Santa Cruz, CA, United States), washed three times, followed by incubation with the corresponding horseradish peroxidase-conjugated secondary antibodies (1:1000). Immunoreactive bands were visualized by chemiluminescence detection (Milipore Corp., Billerica, MA, United States) and analysed by densitometric analysis using the ImageJ software (version 1.30v; National Institutes of Health Research Services Branch, Bethesda, MD, United States). The ANXA2 protein level is expressed as relative ratio, which was calculated as signal intensity (SI) of ANXA2 divided by SI of β-actin[19].

Immunofluorescence assay

Cells (1×10^6) were plated on cover slips and cultured for 24 h in 24-well plates. After three washes with phosphate-buffered saline (PBS), the cells were fixed with 4% paraformaldehyde for 10 min and blocked with 3% BSA in PBS for 30 min at 37 ℃. Then, the samples were incubated overnight at 4 ℃ with the anti-ANXA2 (1:100). After three washes with PBS, the samples were incubated for 1 h at 37 ℃ in the dark with the corresponding Cy3-labeled goat anti-rabbit immunoglobulin G (IgG) secondary antibody (1:500; Beyotime Institute of Biotechnology), washed three times with PBS, stained with 4,6-diamidino-2-phenylindole for 5 min, washed three times with PBS, and sealed with 50% glycerine. The immunostaining analysis was conducted by an multifunction microscope (IX71; Olympus Corp., Tokyo, Japan).

Cell proliferation assay

Cell proliferation was evaluated using the cell counting kit-8 (CCK-8; Beyotime Institute of Biotechnology) and following the manufacturer's instructions. MHCC97-H (untransfected), MHCC97-H/control-shRNA and MHCC97-H/ANXA2-shRNA cells were seeded in 96-well plates (2×10^3 cells/well in 100 μL medium) and cultured for 24 h. Wells with medium alone (no cells) served as blank controls. CCK-8 solution (10 μL/well) was added to the culture medium and incubated for 2 h, after which the A_{450} was measured by a microplate reader (Synergy HT; BioTek Corp., Winooski, VT, United States) at various time points. Experiments were performed in triplicate.

Cell cycle assay

Cell cycle assay was performed using the cell cycle and apoptosis analysis kit (Beyotime Institute of Biotechnology) and following the manufacturer's instructions. MHCC97-H (untransfected), MHCC97-H/control-shRNA and MHCC97-H/ANXA2-shRNA cells were seeded in 6-well plates (1.0×10^6 cells/well in 2 mL medium). After 24 h of culturing, the cells were digested with trypsin enzyme, washed with pre-cooled PBS, and fixed in pre-cooled 70% ethanol for 24 h at 4 ℃. The cells were then stained with propidium iodide and analysed by flow cytometry (FACSCalibur; Becton Dickinson Medical Devices Co Ltd., Shanghai, China) to determine the cell cycle distribution. Experiments were performed in triplicate[20].

Transwell assay

MHCC97-H (untransfected), MHCC97-H/control-shRNA

and MHCC97-H/ANXA2-shRNA cells were plated at 1.0×10^5 cells/well in 0.5 mL of serum-free medium in 24-well matrigel-coated transwell units with polycarbonate filters (8 μm pore size; Costar Inc., Milpitas, CA, United States). The outer chambers were filled with 0.5 mL of medium supplemented with 10% FBS. After 24 h, the cells were fixed in methanol and stained with crystal violet. The top surface of the membrane was gently scrubbed with a cotton bud, and the cells that had invaded through the membrane filters were counted. The invasion inhibition rate (%) was calculated as [(A - B)/A) × 100], where A was the invading cells' percentage for the MHCC97-H group and B was the invading cells' percentage for the MHCC97-H/ANXA2-shRNA group.

In vitro wound-healing assay

The various HCC cell types were cultured in 12-well plates; at subconfluency, the cell monolayer was scratched (wound) with a plastic pipette tip, washed with serum-free medium, and cultured in DMEM medium supplemented with 0.1% FBS. The relative migration distance (%) travelled at various time points (0 and 8 h) was calculated as [(Ax - Bx)/(A_{mock} - B_{mock}) × 100%], where A was the wound width prior to incubation and B was the wound width after incubation[21].

Xenograft tumour-growth assay

The animal protocol was approved by the Ethical Review Committee for Animal Experimentation of Nantong University (China). Specific-pathogen free BALB/C nude mice (6-wk-old and 20 ± 3 g; Super-B and K Laboratory Animal Co., Ltd., Shanghai, China) were randomly assigned to three groups for xenografting of MHCC97-H (untransfected; $n = 4$), MHCC97-H/control-shRNA ($n = 4$), and MHCC97-H/ANXA2-shRNA ($n = 4$) cells. For each group, right flank subcutaneous injection was made with 2×10^7 of the respective HCC cells suspended in 0.2 mL of DMEM medium. Four mice injected with normal saline alone represented the control (non-xenografted) group. Over 21 d of growth, tumour size was routinely measured using callipers and used to calculate the tumour volume by the formula: [(length × width^2)/2]. On post-injection day 21, the animals were sacrificed for liver excision and complete tumour resection. The tumorigenicity inhibition rate (%) was calculated for each HCC-xenografted group as [(tumour $weight_{control}$ - tumour $weight_{shRNA}$)/tumour $weight_{control}$) × 100][22].

Histopathological examination of resected xenografted tumours

Resected tissues were processed for haematoxylin and eosin staining by dehydrating, sectioning (3 μm thick), and mounting on glass slides. For analysis, the sections were rehydrated in distilled water for 2 min, stained with haematoxylin for 5 min, washed with tap water three times for 5 min each, dehydrated with 95% ethanol for 5 s stained with eosin for 2 min, washed with 70% ethanol two times for 5 min each, and air dried.

Immunohistochemical examination of resected xenografted tumours

Resected tissues were processed for were immunohistochemical analysis by formalin fixing, embedding in paraffin, sectioning (3 μm thick), and mounting on glass slides. For analysis, the sections were deparaffinised by soaking in xylene for two times at 10 min each, dehydrated by soaking in an ethanol to distilled water gradient for 5 min at each serial dilution, washed with PBS (pH 7.4) three times, and incubated in endogenous peroxidase blocking solution for 5 min (Immunostain EliVision Kit; Maixin Biotech Inc., Fuzhou, China). The treated sections were subjected to antigen-retrieval by boiling in 0.01 mol/L citrate buffer (pH 6.0) for 10 min (650 W microwave) and blocking of non-specific antibody binding by pretreatment with 0.5% BSA in PBS. After rinsing with PBS, the processed sections were incubated overnight at 4 ℃ with ANXA2 antibody (1:500), washed three times with 0.05% Tween-20 in PBS, and stained with the chromogen 3, 3'-diaminobenzidine tetrahydrochloride. The slide was then rinsed with distilled water, counterstained with haematoxylin, dehydrated, and air-dried. Negative control sections were generated by the same procedure except that the non-specific mouse IgG antibody was used. All samples were evaluated by light microscope by an expert who was blinded to the group and outcome. ANXA2 staining intensity is expressed as an immunoreactive score[23].

Statistical analysis

Results are expressed as mean ± SD. Significance of differences detected between groups was assessed by one-way analysis of variance followed by the least significant difference test or Newman-Keuls test. A P value of < 0.05 was set as the threshold of significance.

RESULTS

ANXA2 is over-expressed in HCC cells

As shown in Figure 1A, the ANXA2 protein level detected in MHCC97-H cells was the highest among the four HCC cell lines and was 8-times higher ($P < 0.05$) than that detected in the normal cell line LO2. Additionally, the level of ANXA2 mRNA expression was significantly higher in the MHCC97-H cells than that in the other HCC cells and the LO2 cells (Table 1; $P < 0.001$). Thus, the MHCC97-H cell line was selected for subsequent study of the effects of shRNA targeting ANXA2 on cell invasion, migration, and tumorigenic potential of hepatoma cells.

ANXA2 expression in MHCC97-H cells is inhibited by shRNA in vitro

The silencing efficiency of ANXA2-specific shRNA in MHCC97-H cells reached approximately 80%. As shown in Table 2 and Figure 1B, the expression levels of ANXA2 mRNA and protein were significantly lower in the MHCC97-H/ANXA2-shRNA cells than in the MHCC97-H/control-shRNA cells and in the MHCC97-H

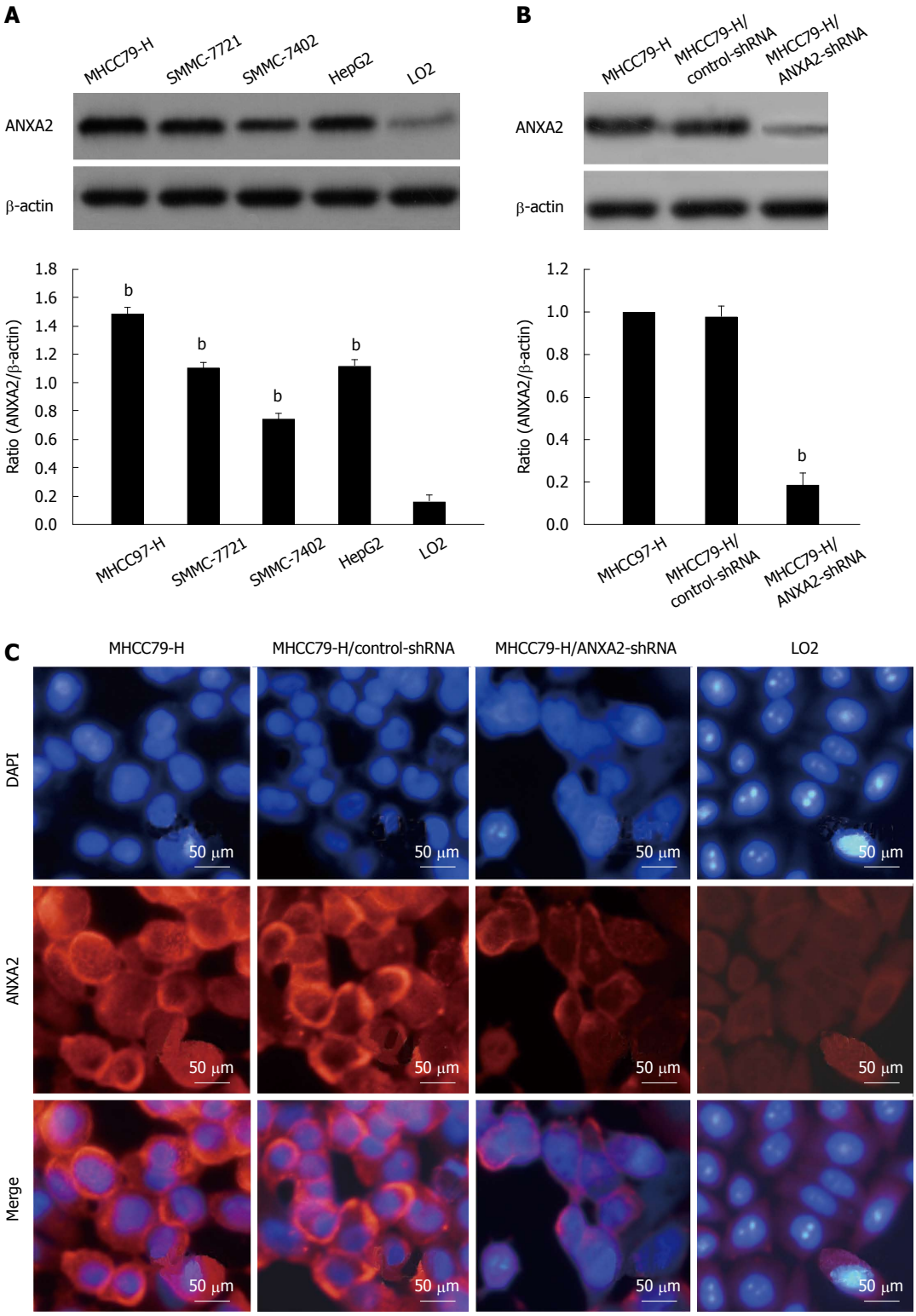

Figure 1 Annexin A2 expression level in hepatoma cells and silencing efficiency of small hairpin RNA in MHCC97-H cells. A: Representative Western blotting images of hepatocellular carcinoma cell lines and the normal hepatic cell line LO2. $^{b}P < 0.01$ *vs* LO2; B: Representative Western blotting images of annexin A2 (ANXA2) silencing upon transfection of small hairpin RNA (shRNA). $^{b}P < 0.01$ *vs* MHCC97-H; C: Representative immunofluorescence images of ANXA2 cellular distribution (× 400). DAPI: 4,6-diamidino-2-phenylindole.

(untransfected) cells. The levels detected in the MHCC97-H/control-shRNA cells and MHCC97-H cells were not significantly different. As shown in Figure 1C, ANXA2 (red fluorescence) expression in the MHCC97-H cells was mainly localized to the cellular membrane and cytoplasm, and some localization was detected in the nucleus. The MHCC97-H/ANXA2-shRNA cells showed obviously lower density of the red immunofluorescent signal

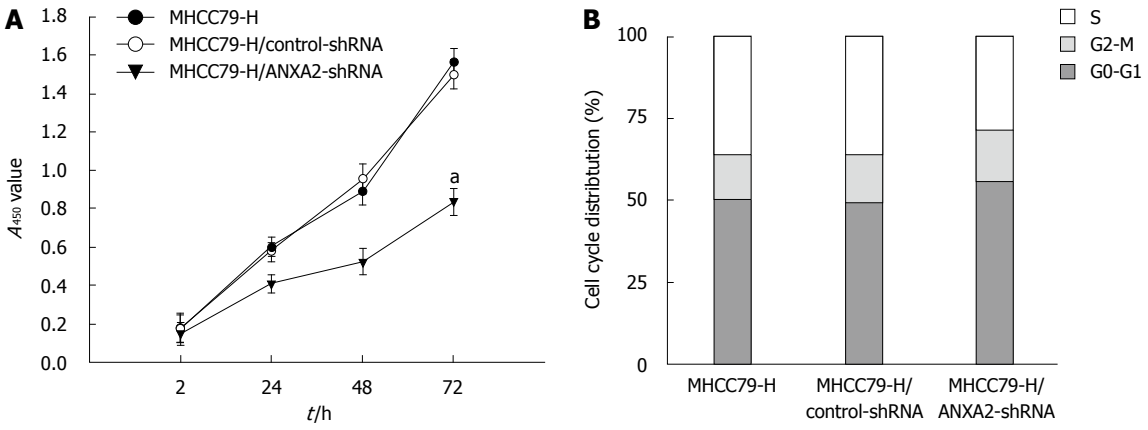

Figure 2 Effect of small hairpin RNA-mediated annexin A2 silencing on proliferation and cell cycling of MHCC97-H cells. A: Cellular proliferation assay. [a]*P* < 0.05 *vs* the A_{450} of MHCC97-H cells at 72 h; B: Cell cycle assay. *P* < 0.05 for percentage of MHCC97-H/annexin A2 (ANXA2)-small hairpin RNA (shRNA) cells in S phase *vs* that of MHCC97-H cells.

Table 1 Expression level of ANXA2 mRNA in hepatocellular carcinoma cells and normal hepatic cells

Group	*n*	Ct_{ANXA2}	$Ct_{\beta\text{-actin}}$	$2^{-\Delta\Delta Ct}$
LO2	5	25.16 ± 0.09	20.86 ± 0.03	1.00
HepG2	5	22.14 ± 0.15	20.66 ± 0.02	7.07 ± 0.35[b]
SMMC-7402	5	22.87 ± 0.15	20.80 ± 0.14	4.68 ± 0.31[b]
SMMC-7721	5	22.21 ± 0.12	20.72 ± 0.10	7.02 ± 0.19[b]
MHCC97-H	5	21.85 ± 0.26	20.78 ± 0.13	9.45 ± 0.53[b]

[b]*P* < 0.001 *vs* the LO2 group.

Table 2 Inhibition of ANXA2 mRNA expression by small hairpin in MHCC97-H cells

Group	*n*	Ct_{ANXA2}	$Ct_{\beta\text{-actin}}$	$2^{-\Delta\Delta Ct}$
MHCC97-H	5	21.84 ± 0.11	20.77 ± 0.16	1.00
MHCC97-H/control-shRNA	5	21.83 ± 0.21	20.72 ± 0.10	0.97 ± 0.04
MHCC97-H/ANXA2-shRNA	5	24.24 ± 0.55	20.80 ± 0.14	0.20 ± 0.05[b]

[b]*P* < 0.001 *vs* the MHCC97-H group. shRNA: Small hairpin RNA.

in the cellular membrane and cytoplasm, as compared to both MHCC97-H and MHCC97-H/control-shRNA cells. Thus, the ANXA2-shRNA was capable of down-regulating ANXA2 expression. Intriguingly, the nuclei of the MHCC97-H/ANXA2-shRNA cells (blue fluorescence) showed signs of early apoptosis (fragmentation with condensed chromatin), as compared to the nuclei of the MHCC97-H cells or the MHCC97-H/control-shRNA cells.

ANXA2 deficiency inhibits proliferation of MHCC97-H cells in vitro

The effects of ANXA2 deficiency on proliferation and cell cycling of MHCC97-H cells are shown in Figure 2. At 72 h post-transfection, the MHCC97-H/ANXA2-shRNA cells showed significantly lower proliferation potential than the MHCC97-H cells or MHCC97-H/control-shRNA cells (*P* < 0.05) (Figure 2A). The proliferation rates of the MHCC97-H cells and the MHCC97-H/control-shRNA cells were not significantly different. The percentage of MHCC97-H/ANXA2-shRNA cells in S phase was significantly lower than that in the MHCC97-H cells (27.76% *vs* 36.14%, *P* < 0.05), whereas the percentages of MHCC97-H/ANXA2-shRNA cells in G_0-G_1 phase and G_2-M phase were significantly higher than those in the MHCC97-H cells (both *P* < 0.05) (Figure 2B). Thus, shRNA targeted suppression of ANXA2 inhibits the growth of MHCC97-H/shRNA cells *in vitro*.

ANXA2 silencing suppresses the invasion and migration potential of MHCC97-H cells in vitro

As shown in Figure 3, the invasive potential of MHCC-97-H/ANXA2-shRNA cells was significantly lower than that of the MHCC97-H cells (52.16% *vs* 86.14%, *P* < 0.05). The invasion inhibition rate in MHCC97-H/ANXA2-shRNA cells reached up to 39.45%. In addition, the migration potential of MHCC97-H/ANXA2-shRNA cells was significantly lower than that of the MHCC97-H cells (63.49% *vs* 100%, *P* < 0.05). The migration inhibition rate in MHCC97-H/ANXA2-shRNA cells reached up to 36.51%. The migration inhibition rates of the MHCC97-H cells and the MHCC97-H/control-shRNA cells were not significantly different.

Down-regulation of ANXA2 inhibits xenograft tumour growth in vivo

As shown in Figure 4A, the tumour volumes of MHCC-97-H/ANXA2-shRNA xenograft group were remarkably smaller than those of the MHCC97-H xenograft group or the MHCC97-H/control-shRNA xenograft group. Unlike the non-xenografted group (Figure 4A), all three xenografted groups showed obvious emaciation, especially the MHCC97-H group and the MHCC97-H/control-shRNA group. As shown in Figure 4B, by day 21 after cell injection the average tumour weight for the MHCC97-H/ANXA2-shRNA group was distinctly lower than that for either the MHCC97-H group or the MHCC97-H/control-shRNA group (both *P* < 0.05). The shRNA-mediated inhibition rate of xenografted tumours reached 38.2%. The

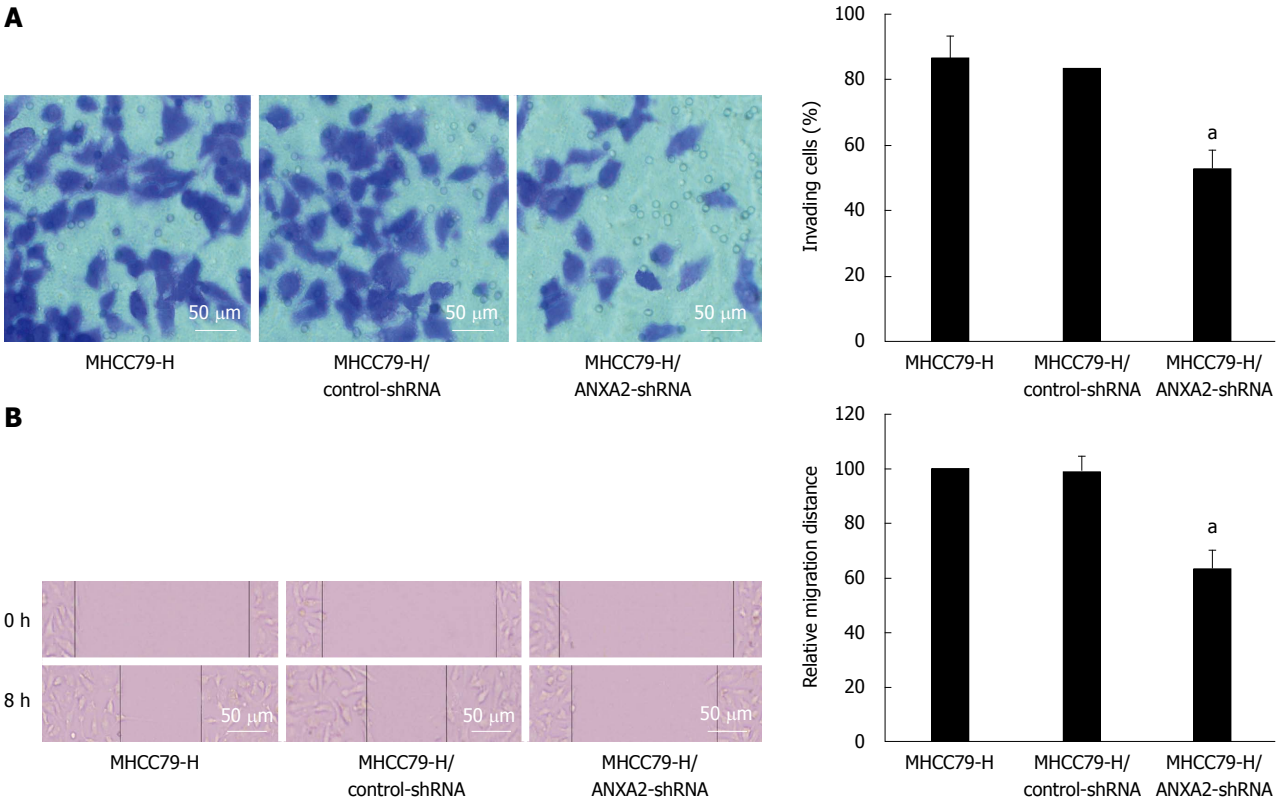

Figure 3 Suppressive effect of small hairpin RNA -mediated annexin A2 silencing on the invasion and migration potential of MHCC97-H cells. A: Representative images of invasive cells (stained with crystal violet) from: the MHCC97-H group; the MHCC97-H/control-small hairpin RNA (shRNA) group; the MHCC97-H/annexin A2 (ANXA2)-small hairpin RNA (shRNA) group; B: Representative images of cell migration. [a]*P* < 0.05 *vs* MHCC97-H cells.

Table 3 Intensity of ANXA2 expression in xenograft tumours

Group	*n*	ANXA2 intensity				*Z*
		-	+	++	+++	
MHCC97-H	4	0	0	0	4	
MHCC97-H/control-shRNA	4	0	0	1	3	1.000
MHCC97-H/ANXA2-shRNA	4	1	3	0	0	2.530[a]

[a]*P* < 0.05 *vs* the MHCC97-H group. shRNA: Small hairpin RNA.

tumour growth curve over 21 d indicated that ANXA2 silencing in MHCC97-H cells reduced their tumorigenic potential *in vivo* (Figure 4C).

As shown in Figure 4D, the morphological characteristics of the xenograft tumours derived from MHCC97-H/ANXA2-shRNA cells were not fundamentally different from the tumours derived from the other cell types. Similar to the *in vitro* observations, ANXA2 expression was mainly localized to the cellular membrane in the MHCC97-H/ANXA2-shRNA tumour tissues and to both the cellular membrane and cytoplasm in the MHCC97-H tumour tissues and the MHCC97-H/control-shRNA tumour tissues. Moreover, the ANXA2 expression level in the xenograft tumours of the MHCC97-H/ANXA2-shRNA group was significantly lower than that in the xenograft tumours of the MHCC97-H group (Table 3). The ANXA2 expression levels in the xenograft tumours of the MHCC97-H group and the MHCC97-H/control-shRNA group were not significantly different.

DISCUSSION

In the present study ANXA2 was found to be up-regulated in HCC cells, particularly those with high metastasis potential and invasion ability. Furthermore, shRNA-mediated silencing of ANXA2 was shown to inhibit the invasion, migration, and tumorigenic potential of hepatoma cells. These results not only provide further insight into the pathogenic mechanisms of HCC, but also suggest ANXA2 as a potential target of future molecular therapies.

Enhanced expression and activation of ANXA2 in cancerous tissues has been reported for many different tumour types, including HCC[14,24,25], which led investigators to consider the potential anti-tumour benefit of inhibiting its gene expression or protein phosphorylation. Knockdown of ANXA2 in glioma cells led to a remarkable decrease in tumour size and suppression of tumour progression and proliferation[26]. Similarly, our results showed that the proliferation ability of MHCC97-H/ANXA2-shRNA cells was significantly suppressed both *in vitro* and *in vivo*. In another previous study of non-small cell lung cancer (NSCLC), ANXA2 knockdown in human adenocarcinoma A_{549} cells led to defective proliferation *in vitro* and reduced tumour growth *in vivo*; additionally, the knockdown cells were arrested at the G2 phase[27]. In the current study, MHCC97-H cells with shRNA-mediated silencing of ANXA2 showed a significantly lower percentage of cells in the S phase than the MHCC97-H cells

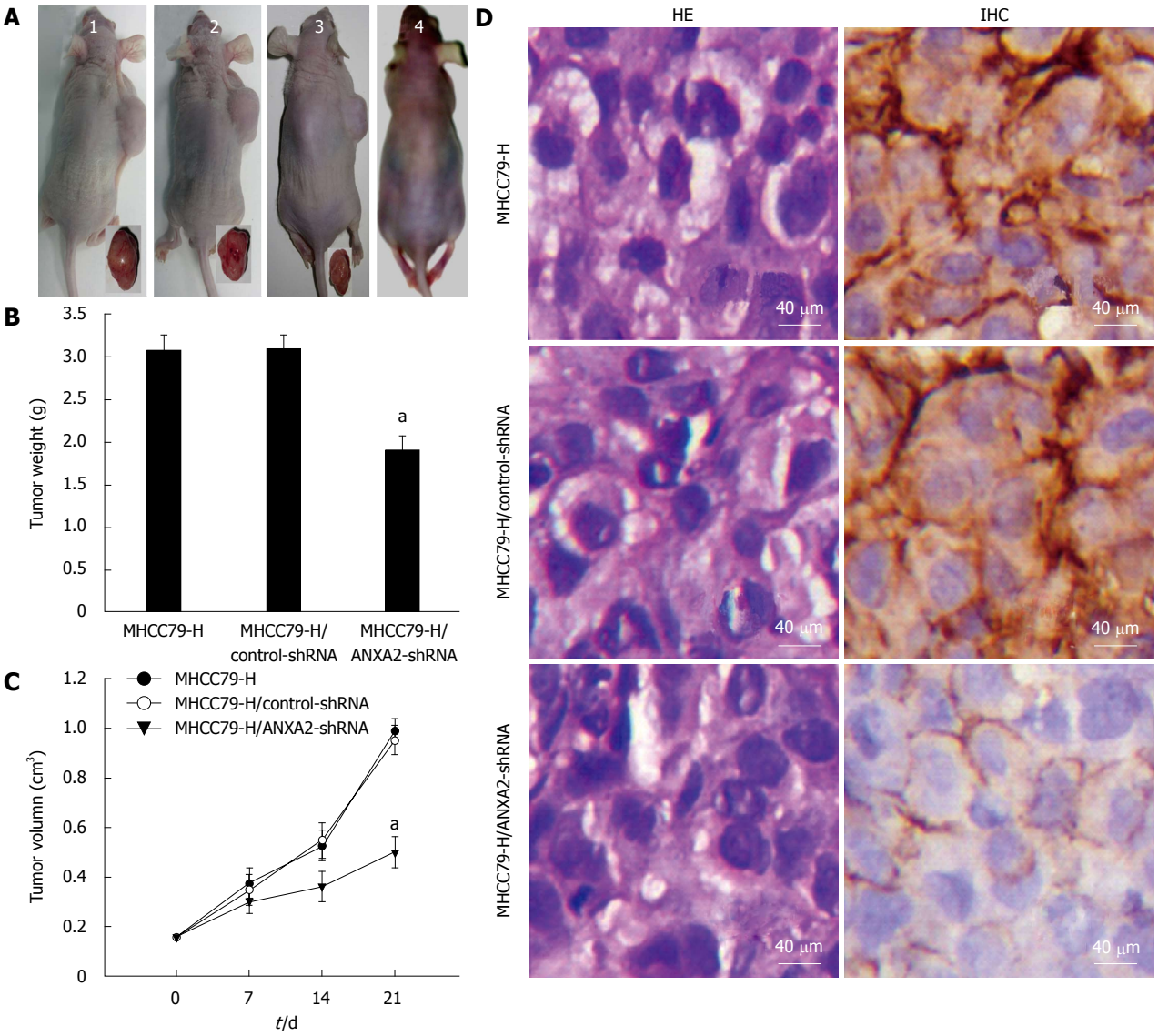

Figure 4 Inhibitive effect of small hairpin RNA-mediated annexin A2 silencing on xenograft tumour growth *in vivo*. A: Representative images of xenografted and control mice and resected tumours. The MHCC97-H (untransfected) group (1); the MHCC97-H/control-small hairpin RNA (shRNA) group (2); the MHCC97-H/annexin A2 (ANXA2)-shRNA group (3); the blank control group (4). Tumorigenic nude mice appeared obviously emaciated, especially the those in the MHCC97-H group and MHCC97-H/control-shRNA group; B: Average tumour weights. $^{a}P < 0.05$ *vs* MHCC97-H group; C: Tumour growth rates. $^{a}P < 0.05$ *vs* MHCC97-H group at post-injection day 21; D: Representative immunohistochemical analysis and hematoxylin and eosin staining results (× 400). The density of ANXA2 staining (brown) in the cytoplasm of MHCC97-H/ANXA2-shRNA cells was obviously lower than that for the MHCC97-H cells or the MHCC97-H/control-shRNA cells. ANXA2 was mainly localized in the membrane of the MHCC97-H/ANXA2-shRNA cells, and localized in both the membrane and cytoplasm of the MHCC97-H cells and the MHCC97-H/control-shRNA cells. The morphological characteristics of subcutaneous xenograft tumours derived from MHCC97-H/ANXA2-shRNA cells were not fundamentally different from the other tumours.

with endogenously enhanced ANXA2. This results from both studies indirectly indicate a promising anti-proliferative effect for ANXA2 silencing.

While previous studies have shown that increased ANXA2 levels are associated with enhanced tumour cell proliferation and HCC development[21,27], our study achieved a relatively low inhibition of tumour growth upon ANXA2 silencing. In the NSCLC study described above, the downstream effects of ANXA2 silencing were explored and a significant effect on p53 expression was discovered[27]. It is possible that ANXA2 may facilitate cell proliferation partly through the regulation of p53 *via* JNK/c-Jun in HCC, since disruption of the p53/miRNA-34 axis has been shown to result in abnormal apoptosis and tumour progression[28]. Furthermore, since ANXA2 is only one of the increased proteins in HCC[1,2], ANXA2 deficiency is expected to only partly, rather than wholly, suppress tumour growth.

Previous molecular studies have determined that ANXA2 promotes invasion and migration of human HCC cells *in vitro via* its interaction with HAb18G/CD147[18,21]. Depletion of HAb18G/CD147 produced a rounded morphology, which is associated with amoeboid movement, while depletion of ANXA2 resulted in an elongated morphology, which is associated with mesenchymal movement. HAb18G/CD147 was also found to promote

cell motility of HCC cells by regulating ANXA2-activated RhoA and Rac1 signalling pathways[18,21]. Plasmin, a downstream factor of ANXA2 activity, is essential for metastatic progression due to its activation of metalloproteinases and degradation of extracellular matrix components[10,29]. In another previous study of human adenomyosis, ANXA2 was shown to function as a key mediator of metastasis and proangiogenesis of endometrial cells[30]. Accumulating evidence has suggested that interactions between ANXA2 and its binding partners contribute to the tumour microenvironment, and together act to enhance metastasis[10]. Our observations of ANXA2 silencing suppressing the invasion and migration potential of hepatoma cells suggest that the invasion and migration potential of HCC cells are correlated with ANXA2 expression level. Furthermore, our finding that ANXA2 silencing is sufficient to inhibit invasion of HCC cells support the notion that ANXA2 is a potential therapeutic target for treating tumour development (through angiogenesis) and progression (through metastasis)[31,32].

The effects of ANXA2 on p53 may modulate apoptotic processes, which are critically associated with cell survival and may also have effects on proliferation[33]. Additionally, ANXA2 has been characterized as one of the factor H ligands binding to apoptotic cells, and has been shown to promote cell apoptosis in systemic lupus erythematosus *via* this mechanism[34]. In the current study, obvious apoptosis was observed in MHCC97-H/ANXA2-shRNA, suggesting that ANXA2-shRNA could suppress the proliferation and invasion ability of hepatoma cells with high metastasis potential, possibly by promoting cell apoptosis. In a previous study of the expression characteristics and diagnostic value of ANXA2 in HCC, we discovered an intermediate state of ANXA2 level in HCC adjacent tissue[35]. In the current study, we defined the distribution profile of ANXA2 expression in HCC cells, with the primary localization occurring in the cell membrane and cytoplasm and some localization occurring in the nucleus.

In conclusion, the results presented herein suggest that ANXA2 is up-regulated in HCC cells with high metastasis potential and invasion ability, and demonstrated that shRNA-mediated silencing of ANXA2 inhibits the invasion, migration, and tumorigenic potential of HCC cells. Collectively, these data reveal a link between the level of ANXA2 expression and HCC metastasis, as well as suggest the potential utility of ANXA2 as a predictive biomarker for HCC prognosis and as a therapeutic target of molecular-based strategies. It, therefore, will be important to carry out further investigations to identify additional signalling modulators and to delineate pivotal regulatory mechanisms involving ANXA2 and HCC metastasis.

COMMENTS

Background

Cell invasion and tumour progression remain two of the major obstacles that must be overcome before hepatocellular carcinoma (HCC) is finally conquered. Annexin A2 (ANXA2) is a 36-kDa calcium-dependent, phospholipid-binding protein expressed on various cell types. In addition, ANXA2 expression is up-regulated in various tumour types, where it plays multiple roles in tumorigenesis and development.

Research frontiers

Up-regulated ANXA2 expression has been detected in clinical samples of HCC, and ANXA2 phosphorylation has been demonstrated as essential for invasion and metastasis of pancreatic cancer. Moreover, the mechanism by which ANXA2 promotes tumour metastasis has been defined as induction of the conversion of plasminogen to plasmin. However, the effect of small hairpin RNA targeting ANXA2 on biological behaviours of hepatoma cells has not yet been reported. In the present study, ANXA2 overexpression was found in MHCC97-H cells, a novel HCC cell line with high metastasis potential, which was then used to investigate the effects of ANXA2 silencing on cell invasion, migration, and tumorigenic potential of HCC.

Innovations and breakthroughs

This study provides the first reported evidence of endogenous ANXA2 up-regulation in HCC cells with high metastasis potential and invasion ability, and of ANXA2 deficiency inhibiting the invasion, migration, and tumorigenic potential of HCC cells. Collectively, these data not only reveal a link between the level of ANXA2 expression and HCC metastasis, but also indicate the potential utility of this factor as a predictive biomarker for HCC prognosis and as a potential therapeutic target.

Applications

The results provide further insight into the pathogenesis of HCC. These data provide foundational knowledge for further expansion in future studies to identify the additional signalling modulators involved in this pathogenic mechanism. Moreover, the newly identified tumorigenic roles of AXNA2 suggest its utility as a target of anti-metastatic and anti-proliferative therapies.

Peer review

The paper is good design and illustration, deserved to be published.

REFERENCES

1 **Forner A**, Llovet JM, Bruix J. Hepatocellular carcinoma. *Lancet* 2012; **379**: 1245-1255 [PMID: 22353262 DOI: 10.1016/S0140-6736(11)61347-0]

2 **Shen YC**, Hsu C, Cheng CC, Hu FC, Cheng AL. A critical evaluation of the preventive effect of antiviral therapy on the development of hepatocellular carcinoma in patients with chronic hepatitis C or B: a novel approach by using meta-regression. *Oncology* 2012; **82**: 275-289 [PMID: 22555181 DOI: 10.1159/000337293]

3 **DuBray BJ**, Chapman WC, Anderson CD. Hepatocellular carcinoma: a review of the surgical approaches to management. *Mo Med* 2011; **108**: 195-198 [PMID: 21736080]

4 **Lencioni R**, Crocetti L. Local-regional treatment of hepatocellular carcinoma. *Radiology* 2012; **262**: 43-58 [PMID: 22190656 DOI: 10.1148/radiol.11110144]

5 **Vullierme MP**, Paradis V, Chirica M, Castaing D, Belghiti J, Soubrane O, Barbare JC, Farges O. Hepatocellular carcinoma--what's new? *J Visc Surg* 2010; **147**: e1-12 [PMID: 20595072 DOI: 10.1016/j.jviscsurg.2010.02.003]

6 **Hanahan D**, Weinberg RA. Hallmarks of cancer: the next generation. *Cell* 2011; **144**: 646-674 [PMID: 21376230 DOI: 10.1016/j.cell.2011.02.013]

7 **Marquardt JU**, Galle PR, Teufel A. Molecular diagnosis and therapy of hepatocellular carcinoma (HCC): an emerging field for advanced technologies. *J Hepatol* 2012; **56**: 267-275 [PMID: 21782758 DOI: 10.1016/j.jhep.2011.07.007]

8 **Sia D**, Villanueva A. Signaling pathways in hepatocellular carcinoma. *Oncology* 2011; **81** Suppl 1: 18-23 [PMID: 22212931 DOI: 10.1159/000333254]

9 **Teufel A**, Marquardt JU, Galle PR, Wörns M. [Hepatocellular carcinoma: what's new?]. *Dtsch Med Wochenschr* 2012; **137**: 210-213 [PMID: 22250042 DOI: 10.1055/s-0031-1292890]

10 **Lokman NA**, Ween MP, Oehler MK, Ricciardelli C. The role of annexin A2 in tumorigenesis and cancer progression. *Cancer Microenviron* 2011; **4**: 199-208 [PMID: 21909879 DOI:

10.1007/s12307-011-0064-9]
11 **Madureira PA**, Surette AP, Phipps KD, Taboski MA, Miller VA, Waisman DM. The role of the annexin A2 heterotetramer in vascular fibrinolysis. *Blood* 2011; **118**: 4789-4797 [PMID: 21908427 DOI: 10.1182/blood-2011-06-334672]
12 **Gerke V**, Moss SE. Annexins: from structure to function. *Physiol Rev* 2002; **82**: 331-371 [PMID: 11917092]
13 **Flood EC**, Hajjar KA. The annexin A2 system and vascular homeostasis. *Vascul Pharmacol* 2011; **54**: 59-67 [PMID: 21440088 DOI: 10.1016/j.vph.2011.03.003]
14 **Mohammad HS**, Kurokohchi K, Yoneyama H, Tokuda M, Morishita A, Jian G, Shi L, Murota M, Tani J, Kato K, Miyoshi H, Deguchi A, Himoto T, Usuki H, Wakabayashi H, Izuishi K, Suzuki Y, Iwama H, Deguchi K, Uchida N, Sabet EA, Arafa UA, Hassan AT, El-Sayed AA, Masaki T. Annexin A2 expression and phosphorylation are up-regulated in hepatocellular carcinoma. *Int J Oncol* 2008; **33**: 1157-1163 [PMID: 19020748]
15 **Zheng L**, Foley K, Huang L, Leubner A, Mo G, Olino K, Edil BH, Mizuma M, Sharma R, Le DT, Anders RA, Illei PB, Van Eyk JE, Maitra A, Laheru D, Jaffee EM. Tyrosine 23 phosphorylation-dependent cell-surface localization of annexin A2 is required for invasion and metastases of pancreatic cancer. *PLoS One* 2011; **6**: e19390 [PMID: 21572519 DOI: 10.1371/journal.pone.0019390]
16 **Ohno Y**, Izumi M, Kawamura T, Nishimura T, Mukai K, Tachibana M. Annexin II represents metastatic potential in clear-cell renal cell carcinoma. *Br J Cancer* 2009; **101**: 287-294 [PMID: 19513064 DOI: 10.1038/sj.bjc.6605128]
17 **Sharma M**, Ownbey RT, Sharma MC. Breast cancer cell surface annexin II induces cell migration and neoangiogenesis via tPA dependent plasmin generation. *Exp Mol Pathol* 2010; **88**: 278-286 [PMID: 20079732 DOI: 10.1016/j.yexmp.2010.01.001]
18 **Zhao P**, Zhang W, Tang J, Ma XK, Dai JY, Li Y, Jiang JL, Zhang SH, Chen ZN. Annexin II promotes invasion and migration of human hepatocellular carcinoma cells in vitro via its interaction with HAb18G/CD147. *Cancer Sci* 2010; **101**: 387-395 [PMID: 20047591 DOI: 10.1111/j.1349-7006.2009.01420.x]
19 **Zhang HJ**, Li C, Zhang GY. ATPA induced GluR5-containing kainite receptor S-nitrosylation via activation of GluR5-Gq-PLC-IP(3)R pathway and signalling module GluR5·PSD-95·nNOS. *Int J Biochem Cell Biol* 2012; **44**: 2261-2271 [PMID: 23000395]
20 **Gao J**, Zhu J, Li HY, Pan XY, Jiang R, Chen JX. Small interfering RNA targeting integrin-linked kinase inhibited the growth and induced apoptosis in human bladder cancer cells. *Int J Biochem Cell Biol* 2011; **43**: 1294-1304 [PMID: 21601006 DOI: 10.1016/j.biocel.2011.05.003]
21 **Zhao P**, Zhang W, Wang SJ, Yu XL, Tang J, Huang W, Li Y, Cui HY, Guo YS, Tavernier J, Zhang SH, Jiang JL, Chen ZN. HAb18G/CD147 promotes cell motility by regulating annexin II-activated RhoA and Rac1 signaling pathways in hepatocellular carcinoma cells. *Hepatology* 2011; **54**: 2012-2024 [PMID: 21809360 DOI: 10.1002/hep.24592]
22 **Ruan J**, Liu F, Chen X, Zhao P, Su N, Xie G, Chen J, Zheng D, Luo R. Inhibition of glypican-3 expression via RNA interference influences the growth and invasive ability of the MHCC97-H human hepatocellular carcinoma cell line. *Int J Mol Med* 2011; **28**: 497-503 [PMID: 21617840]
23 **Wang D**, Xu MR, Wang T, Li T, Zhu Jw. MTSS1 overexpression correlates with poor prognosis in colorectal cancer. *J Gastrointest Surg* 2011; **15**: 1205-1212 [PMID: 21562916 DOI: 10.1007/s11605-011-1546-2]
24 **Wu B**, Zhang F, Yu M, Zhao P, Ji W, Zhang H, Han J, Niu R. Up-regulation of Anxa2 gene promotes proliferation and invasion of breast cancer MCF-7 cells. *Cell Prolif* 2012; **45**: 189-198 [PMID: 22452352 DOI: 10.1111/j.1365-2184.2012.00820.x]
25 **Gould KL**, Woodgett JR, Isacke CM, Hunter T. The protein-tyrosine kinase substrate p36 is also a substrate for protein kinase C in vitro and in vivo. *Mol Cell Biol* 1986; **6**: 2738-2744 [PMID: 2946940]
26 **Zhai H**, Acharya S, Gravanis I, Mehmood S, Seidman RJ, Shroyer KR, Hajjar KA, Tsirka SE. Annexin A2 promotes glioma cell invasion and tumor progression. *J Neurosci* 2011; **31**: 14346-14360 [PMID: 21976520 DOI: 10.1523/JNEUROSCI.3299-11.2011]
27 **Wang CY**, Chen CL, Tseng YL, Fang YT, Lin YS, Su WC, Chen CC, Chang KC, Wang YC, Lin CF. Annexin A2 silencing induces G2 arrest of non-small cell lung cancer cells through p53-dependent and -independent mechanisms. *J Biol Chem* 2012; **287**: 32512-32524 [PMID: 22859294]
28 **Cha YH**, Kim NH, Park C, Lee I, Kim HS, Yook JI. MiRNA-34 intrinsically links p53 tumor suppressor and Wnt signaling. *Cell Cycle* 2012; **11**: 1273-1281 [PMID: 22421157 DOI: 10.4161/cc.19618]
29 **Grieve AG**, Moss SE, Hayes MJ. Annexin A2 at the interface of actin and membrane dynamics: a focus on its roles in endocytosis and cell polarization. *Int J Cell Biol* 2012; **2012**: 852430 [PMID: 22505935]
30 **Zhou S**, Yi T, Liu R, Bian C, Qi X, He X, Wang K, Li J, Zhao X, Huang C, Wei Y. Proteomics identification of annexin A2 as a key mediator in the metastasis and proangiogenesis of endometrial cells in human adenomyosis. *Mol Cell Proteomics* 2012; **11**: M112.017988 [PMID: 22493182]
31 **Sharma MC**, Sharma M. The role of annexin II in angiogenesis and tumor progression: a potential therapeutic target. *Curr Pharm Des* 2007; **13**: 3568-3575 [PMID: 18220793 DOI: 10.2174/138161207782794167]
32 **Zheng L**, Jaffee EM. Annexin A2 is a new antigenic target for pancreatic cancer immunotherapy. *Oncoimmunology* 2012; **1**: 112-114 [PMID: 22720228 DOI: 10.4161/onci.1.1.18017]
33 **Huang Y**, Jin Y, Yan CH, Yu Y, Bai J, Chen F, Zhao YZ, Fu SB. Involvement of Annexin A2 in p53 induced apoptosis in lung cancer. *Mol Cell Biochem* 2008; **309**: 117-123 [PMID: 18008140 DOI: 10.1007/s11010-007-9649-5]
34 **Leffler J**, Herbert AP, Norström E, Schmidt CQ, Barlow PN, Blom AM, Martin M. Annexin-II, DNA, and histones serve as factor H ligands on the surface of apoptotic cells. *J Biol Chem* 2010; **285**: 3766-3776 [PMID: 19951950 DOI: 10.1074/jbc.M109.045427]
35 **Zhang HJ**, Yao DF, Yao M, Huang H, Wu W, Yan MJ, Yan XD, Chen J. Expression characteristics and diagnostic value of annexin A2 in hepatocellular carcinoma. *World J Gastroenterol* 2012; **18**: 5897-5904 [PMID: 23139605 DOI: 10.3748/wjg.v18.i41.5897]

P- Reviewers Mazzanti R, Xu RY **S- Editor** Zhai HH
L- Editor A **E- Editor** Xiong L